

## A MASSIVE COMETARY CLOUD ASSOCIATED WITH IC 1805

MARK H. HEYER, CHRISTOPHER BRUNT, RONALD L. SNELL, JOHN HOWE, AND F. P. SCHLOERB  
Five College Radio Astronomy Observatory, Lederle Research Building, University of Massachusetts, Amherst, MA 01003

JOHN M. CARPENTER  
Institute for Astronomy, University of Hawaii, 2680 Woodlawn Drive, Honolulu, HI 96821

M. NORMANDEAU AND A. R. TAYLOR  
Department of Physics and Astronomy, University of Calgary, 2500 University Drive, NW, Calgary, Alberta, Canada T2N 1N4

P. E. DEWDNEY  
Dominion Radio Astrophysical Observatory, National Research Council, P.O. Box 248, Penticton, BC, Canada, V2A 6K3

Y. CAO  
Department of Physics, California Institute of Technology, Pasadena, CA 91125

AND

S. TEREBEY AND C. A. BEICHMAN  
Infrared Processing and Analysis Center, California Institute of Technology, Pasadena, CA 91125

Received 1996 February 6; accepted 1996 April 4

### ABSTRACT

High-resolution, wide field imaging of  $^{12}\text{CO}$ , 21 cm line and continuum, and *IRAS* far-infrared emissions from the outer Galaxy have identified a massive cometary molecular cloud associated with IC 1805. The dense cloud is remnant molecular material within a large  $10^2$  pc cavity evacuated by the stellar winds and UV radiation field of the cluster O stars. A 37 pc long molecular tail points directly away from the sources of ionizing radiation and is likely due to the effective shielding of radiation by the dense gas and associated dust within the cometary head region. Maps of  $\text{C}^{18}\text{O } J = 1-0$  and  $\text{CS } J = 2-1$  emissions are presented that constrain the column and mean volume densities within the cometary head region to  $10^{22} \text{ cm}^{-2}$  and  $10^4 \text{ cm}^{-3}$ , respectively. A  $1155 L_{\odot}$  point source embedded within the dense gas of the cometary head region provides evidence for ongoing star formation that may have been triggered by shocks driven by the ionization front.

*Subject headings:* ISM: clouds — ISM: globules — ISM: kinematics and dynamics — ISM: molecules — radio continuum: ISM

### 1. INTRODUCTION

In this Letter, we report observations of a large, cometary molecular cloud associated with the open cluster IC 1805 (also OCl 352; Alter, Ruprecht, & Vanysek 1970). The head of the cometary cloud has been previously identified as cloud 7 in the catalog of Sugitani, Fukui, & Ogura (1990), but new observations presented here reveal the existence of a 37 pc long collinear tail that points directly away from the cluster of O stars. The cloud is remnant molecular material associated with the W3-W4-W5 cloud complex and located within a 100 pc cavity in the atomic layer of the Galactic disk (Normandeau, Taylor, & Dewdney 1996a). This void of atomic gas is presumably due to the photoionization and excavation of material by the strong stellar winds and UV radiation fields associated with the massive stars of IC 1805. The UV radiation from the O stars is also responsible for the W4 loop of ionized material (Westerhout 1958). The existence of the molecular cloud within such a harsh environment and the extreme morphology due to its proximity to the stellar sources of ionizing flux provide an opportune region to investigate the effects of massive star formation upon the interstellar gas environment. Observations of  $^{12}\text{CO } J = 1-0$ ,  $\text{C}^{18}\text{O } J = 1-0$ ,  $\text{CS } J = 2-1$ , 21 cm radio continuum, and H I line emission are presented and placed into context with respect to models of dense clouds irradiated by strong photoionizing UV fields (Bertoldi 1989; Bertoldi & McKee 1990; Lefloch & Lazareff 1994). We adopt

a distance of 2350 pc to the W4 region (Massey, Johnson, & DeGioia-Eastwood 1995).

### 2. RESULTS

Data presented in this Letter are part of several ongoing large-scale surveys of the outer Galaxy at various wavelengths that are described in more detail elsewhere (Heyer 1996; Normandeau, Taylor, & Dewdney 1996b; Cao et al. 1996). Images at  $\sim 1'$  resolution of  $^{12}\text{CO}$ , 21 cm continuum, the Palomar Sky Survey Red Plate, H I 21 cm, and *IRAS* HIRES 60 and  $100 \mu\text{m}$  emission from the cometary cloud are shown in Figure 1 (Plate L14). These images provide direct probes of the molecular, ionized, atomic, and dust components of the interstellar environment of the region. The CO map shows an elongated cometary cloud with a bright head that faces the O stars located approximately  $0^{\circ}.4$  toward lower Galactic latitudes. The tail of the cometary cloud extends for  $0^{\circ}.9$  (37 pc) and points directly away from the most luminous O stars within the compact group. The mean full width zero intensity of the tail is  $5'.3$  (3.6 pc). Along the length of the tail, there is little variation of the centroid velocities and of the profile line widths about the respective mean values of  $V_{\text{LSR}}$  of  $-40$  and  $3 \text{ km s}^{-1}$ . Within the head of the cometary cloud, the spectra along the edges are blueshifted by  $2-2.5 \text{ km s}^{-1}$  with respect to the central region. The total CO luminosity,  $L_{\text{CO}}$ , of the cometary cloud is  $860 \text{ K km s}^{-1} \text{ pc}^2$ . Using the factor of Strong

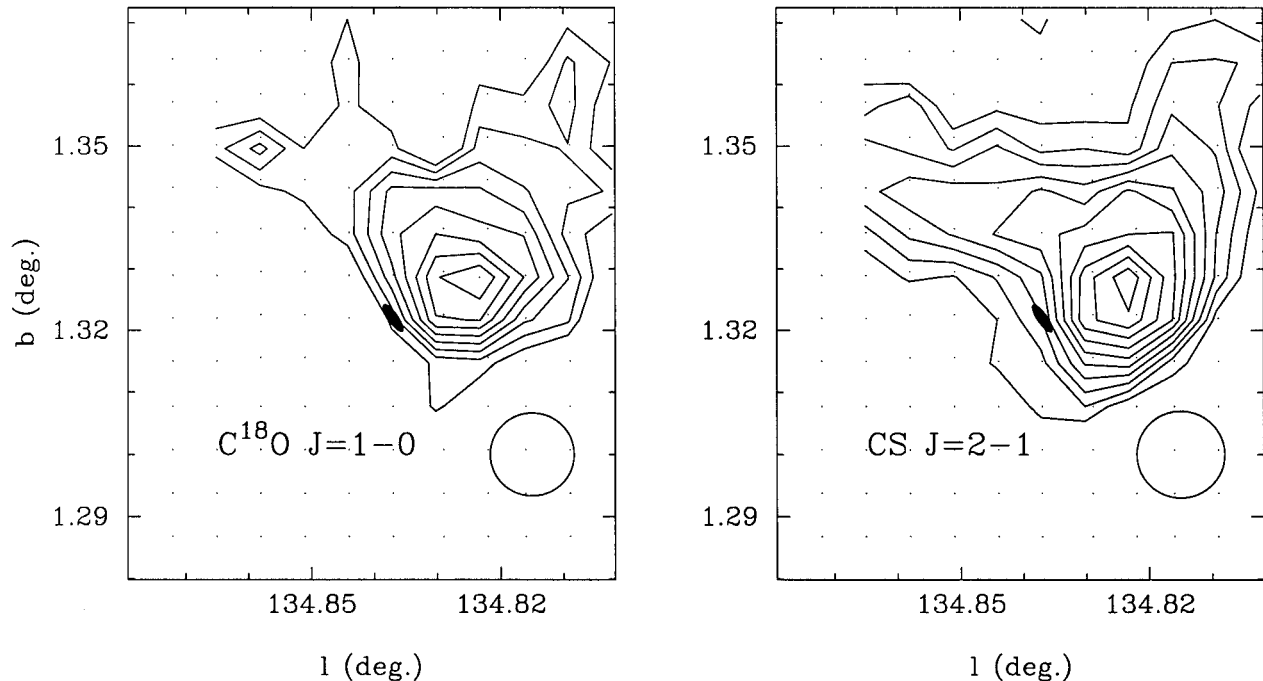


FIG. 2.—Maps of main-beam integrated  $\text{C}^{18}\text{O } J = 1-0$  (left) and  $\text{CS } J = 2-1$  (right) emission. For the  $\text{C}^{18}\text{O}$  map, the contours are 0.6–2.7 spaced by  $0.3 \text{ K km s}^{-1}$ . The contours for the CS map are 0.3–1.8 spaced by  $0.3 \text{ K km s}^{-1}$ . The filled ellipse denotes the location and positional uncertainty (95% confidence level) of IRAS PSC 02310+6133, the small dots show the mapped points, and the circle denotes the observed beam size.

et al. (1988) to convert from  $L_{\text{CO}}$  to total mass, we derive  $5300 M_{\odot}$  for the mass of the cloud. Approximately 64% of the luminosity ( $3400 M_{\odot}$ ) originates within the head of the cometary cloud over a region 6 pc in diameter.

To investigate the distribution of material within the head of the cometary cloud with more direct probes of gas volume and column densities,  $\text{C}^{18}\text{O } J = 1-0$  and  $\text{CS } J = 2-1$  emissions were mapped with the FCRAO 14 m telescope with  $25''$  sampling. These maps are shown in Figure 2. Both maps show a cometary or fan-shaped morphology similar to that seen within the  $^{12}\text{CO}$  image, and the axis of symmetry is oriented identically to that of the  $^{12}\text{CO}$  cometary tail. Assuming that the  $\text{C}^{18}\text{O}$  emissions are optically thin and an excitation temperature of 10 K, we have calculated the LTE  $\text{C}^{18}\text{O}$  column densities for each line of sight. The total  $\text{H}_2$  mass within the  $\text{C}^{18}\text{O}$ -emitting region is  $500 M_{\odot}$  assuming a  $\text{C}^{18}\text{O}$ -to- $\text{H}_2$  abundance ratio of  $1.25 \times 10^{-7}$ . At the head of the cometary cloud, there is approximately  $270 M_{\odot}$  within a 1 pc diameter region. The mean density of this more limited region is  $\approx 1 \times 10^4 \text{ cm}^{-3}$ . Such average densities are consistent with densities required to produce the observed  $\text{CS } J = 2-1$  antenna temperatures. The higher spectral resolution of these data confirm the variations of centroid velocities of the  $^{12}\text{CO}$  profiles. That is, the velocities of the material that fans out from the apex of the cloud are blueshifted by  $1\text{--}1.5 \text{ km s}^{-1}$  relative to the velocities observed along the axis of symmetry.

The 21 cm radio continuum map and POSS image provide direct probes of the associated ionized gas component within this region. The detailed similarities between the radio and optical images suggests that there is very little foreground extinction along these lines of sight, although a patch of visual extinction is associated with the cometary tail. Both images reveal an extended distribution of ionized gas at the edge of the cometary head defined by the CO image. To view the

spatial relationship between the molecular and ionized gas components better, we have overlaid contours of the  $^{12}\text{CO } J = 1-0$  emissions upon the 21 cm continuum image in Figure 3 (Plate L15). The edges of the  $^{12}\text{CO}$ ,  $\text{C}^{18}\text{O}$ , and CS emissions, defined by the respective  $3\sigma$  contours, are coincident with the brightest continuum emission (hereafter, the bright rim) that outlines the periphery of the cometary head. The observed spatial relationship between the ionized and molecular gas components suggests that the enhanced molecular densities are due to compression of material by a shock front that precedes the advancing ionization front (Spitzer 1978).

The 21 cm continuum brightness temperatures at the cometary head range from 6 to 10 K. While the projected source size is 5 pc, the 21 cm continuum emission likely originates from a thin interface layer at the surface of the molecular cloud. An estimate of the thickness of the interface layer is derived from the projected width of the bright rim emission. While not completely resolved by the 21 cm observations, an upper limit to this width is  $0^{\circ}01$  or 0.4 pc. Assuming an electron temperature of  $10^4 \text{ K}$ , the average emission measure along the bright rim is  $4000 \text{ cm}^{-6} \text{ pc}$ , and thus, the density of the ionized gas associated with the cometary head is  $\geq 100 \text{ cm}^{-3}$ . Weaker continuum emission is found within filaments that arch  $0^{\circ}5$  on both sides of the bright rim and connect to more extended nebulosity. There is no ionized gas counterpart to the tail of the cometary cloud at a brightness temperature sensitivity of 1 K. The sensitivity in this region is somewhat compromised by the grating lobes from the nearby bright continuum source W3. Assuming that the  $10^2 \text{ pc}$  excavated zone of the Galactic plane is filled with low-density, ionized material, the observed brightness limit implies a density of  $\leq 3\text{--}4 \text{ cm}^{-3}$  for this region.

There is enhanced H I 21 cm line emission with respect to the H I background at the cometary head and behind the

arched ionized filaments over the velocities at which CO is observed. Enhanced emission is also present along but not coincident with the cometary tail. This atomic gas is likely a result of photodissociation of molecular material by stellar radiation whose wavelength is between 912 and 1109 Å. To quantify the enhanced H I emission more accurately, we have computed a spatially averaged H I spectrum from those lines of sight surrounding the cometary cloud and have subtracted this mean spectrum from all line profiles within the map. The distribution of this residual emission is shown in Figures 1 and 3. The mean velocity of the residual emission is  $-40.6 \text{ km s}^{-1}$ , and the mean width is  $7.3 \text{ km s}^{-1}$ . Assuming that this residual emission reflects atomic gas associated with the CO cloud, we derive a mean atomic gas column density,  $\langle N(\text{H I}) \rangle$ , of  $2.6 \times 10^{20} \text{ cm}^{-2}$  and an H I mass of  $210 M_{\odot}$ .

Finally, far-infrared emission from heated dust grains within the cloud provides another diagnostic of column density and thermal energy flow within the cloud. The *IRAS* Point Source Catalog (1988) identifies the point source PSC 02310+6133 within the cometary head with a spectral energy distribution similar to embedded young stellar objects. The far-infrared luminosity of this object is  $1155 L_{\odot}$ . Diffuse far-infrared emission is located along the lower longitude, ionized, arched filament and is coincident with the H I emission. There is a far-infrared counterpart to the cometary tail. The 60 to  $100 \mu\text{m}$  intensity ratio decreases from 0.55 within the head region to 0.35 within the tail, indicating cooler dust temperatures within the tail.

### 3. DISCUSSION

The cometary cloud identified by CO observations provides an exotic example of remnant molecular material within a large hole of the Galactic plane that has been excavated by the UV radiation and attendant stellar winds from IC 1805. The sharp CO emission gradient at the cometary head, the long, narrow axisymmetric tail pointing away from the stellar cluster, and the presence of ionized and atomic gas coincident with the head attest to the significant effect of the ultraviolet radiation field upon the morphology and evolution of this cloud. Indeed, the very existence of this molecular cloud demonstrates that dense clouds can withstand the harsh radiative conditions generated by massive stars.

Several studies have investigated the effect of a strong, ionizing UV radiation field upon dense clouds within the interstellar environment (Oort & Spitzer 1955; Bertoldi 1989; Bertoldi & McKee 1990; Lefloch & Lazareff 1994). The initial photoionization of the front surface of the cloud creates a strong pressure gradient such that the newly ionized material flows back toward the UV source. As this material recombines, it provides an opacity layer that reduces the amount of incident ionizing flux at the cloud surface. Thus, this ionized boundary layer (IBL) regulates the subsequent propagation of the ionization front into the cloud. For most conditions within the molecular interstellar medium, a shock precedes the ionization front in order to maintain ionization balance. The effect of this shock is to compress the cloud material such that the velocity of the cloud material is less than or equal to the  $D$  critical velocity  $u_D = c_1^2/2c_{\text{II}}$ , where  $c_1$  and  $c_{\text{II}}$  are the sound speeds for the molecular and ionized gas, respectively. Analytical and numerical simulations show that the shock focuses material along the symmetry axis of the cloud, generating a

dense, elongated globule (Bertoldi 1989; Lefloch & Lazareff 1994)

The cometary cloud observed in this study is irradiated by UV flux from the compact group of O stars at a projected distance of 17 pc. Three of the nine O stars account for 90% of the ionizing photons. These are HD 15558 (spectral type O4 III<sub>f</sub>), HD 15570 (O4 I<sub>f</sub>), and HD 15629 (O5 V) (Massey et al. 1995). The rate of ionizing photons  $N_i$  emitted by these three stars is  $2.2 \times 10^{50} \text{ s}^{-1}$  (Panagia 1973). Assuming that the IBL is in ionization equilibrium and is ionization bound, the flux of ionizing photons,  $F_i$ , is given by

$$F_i = \alpha_B \int n_e^2 dl,$$

where  $\alpha_B$  is the recombination rate coefficient and  $\int n_e^2 dl$  is the emission measure. Using the expression for free-free optical depth from Mezger & Henderson (1967), we can relate the emission measure to the radio continuum brightness temperature assuming that the radio emission is optically thin and the temperature of the IBL is  $10^4 \text{ K}$ . Thus, the flux of ionizing photons is given by

$$F_i = 4.9 \times 10^8 T_B \text{ s}^{-1} \text{ cm}^{-2},$$

where  $T_B$  is the radio continuum brightness temperature at 1.42 GHz. This result is independent of the density distribution within the IBL. The brightness temperatures of the bright rim ionization front are  $\sim 8 \text{ K}$ , which imply a flux of ionizing photons of  $4 \times 10^9 \text{ s}^{-1} \text{ cm}^{-2}$  or similar to the flux ( $N_i/4\pi d^2$ ) calculated from the emitted rate of ionizing photons at a projected distance of 17 pc. From this calculation, one can infer that there is little intervening opacity between the emitting stars and the bright rim layer, which is consistent with the low ionized gas densities derived within the void of H I emission. Furthermore, the projected distance must be very close to the true distance between the stars and bright rim which constrains the geometry of the region. The fact that the optical and radio images are so similar also suggests that the illuminating stars are slightly foreground with respect to the observer, so that the front side of the globule is exposed to the UV radiation.

We estimate the factor  $q$  by which the IBL reduces the number of ionizing photons that reach the ionization front:

$$2q = 1 + \left( 1 + \frac{\alpha N_i R_i}{3\pi d^2 c_{\text{II}}^2} \right)^{1/2},$$

where  $\alpha$  is the recombination rate coefficient,  $R_i$  is the radius of curvature of the cloud taken here to be 0.8 pc,  $c_{\text{II}}$  is the ionized gas sound speed, and  $d$  is the distance between the cloud and stellar sources of UV radiation (Spitzer 1978). Evaluating this expression for the cometary cloud assuming an ionized gas sound speed of  $11.4 \text{ km s}^{-1}$ , we find that  $q$  is 33. For comparison,  $4 < q < 6$  for the IC 1396E globule (Serabyn, Güsten, & Mundy 1993) and  $12 < q < 18$  for the globules within the Rosette nebula (Bertoldi 1989). The large value of  $q$  derived in this study with respect to these other clouds reflects the larger radiation field. The insulating boundary layer effectively regulates the transmission of ionizing flux reaching the neutral material and therefore prevents the rapid photoionization of the entire cloud. When  $q$  is known, the ionized gas density at the ionization front can be estimated from the expression  $n_i = F_i/qc_{\text{II}} = 106 \text{ cm}^{-3}$ . This value is

consistent with the lower limit derived from the observed emission measure of the bright rim.

The ionization front is expected to propagate slowly through the cloud at the  $D$ -type critical velocity,  $u_D = 4 \text{ ms}^{-1}$  assuming molecular and ionized gas sound speeds of  $0.3$  and  $11.4 \text{ km s}^{-1}$ , respectively. The velocity of the preceding shock front is  $v_{\text{sh}} = c_{\text{II}}(2\mu_{\text{H II}}n_{\text{II}}/\mu_{\text{H}_2}n_{\text{H}_2})^{1/2}$ , where  $n_{\text{H}_2}$  is the preshock density of the cloud taken here to be  $1000 \text{ cm}^{-3}$  and  $\mu_{\text{H II}}$  and  $\mu_{\text{H}_2}$  are the mean atomic weights for the ionized and molecular gas, respectively. Using the density derived from observations for the ionized gas, and  $\mu_{\text{H II}} = 1.27$ ,  $\mu_{\text{H}_2} = 2.4$ , we calculate a shock velocity at the apex  $v_{\text{sh}} = 3.7 \text{ km s}^{-1}$ . Simulations by Lefloch & Lazareff (1994) show that the magnitude of the shock velocity is largest at the apex and decreases with distance from the axis of symmetry because of the more oblique exposure to the UV field. The velocity difference of the edges of the cometary head are expected to be negative with respect to the apex due to both slower shock velocities and projection of the radial component to the observer. Thus, this relative motion would account for the observed velocity difference between the central and edge regions of the cometary head.

The cometary cloud is distinguished from other cometary globules within strong UV radiation fields not just by its mass but by the  $37 \text{ pc}$  long, axisymmetric tail. Bertoldi & McKee (1990) derive cometary morphologies of equilibrium clouds irradiated by strong UV fields, but these models do not account for the size and the large axial ratio observed for this cloud. Unless all of the motions are in the plane of the sky, the absence of velocity variations along the tail suggests that it is not due to material ablated from the head region and carried downstream. Rather, we propose that the long tail is original cloud material that lies within the shadow cast by the dense, cometary head region and is therefore shielded from the photoionizing and photodissociating radiation field. If such a shadowing condition exists, then the solid angle defined by the far end of the tail and cometary head must constrain the stellar sources of UV radiation. The most luminous stars within the compact group (HD 15558, HD 15570, and HD 15629) lie within this solid angle. From the  $\text{C}^{18}\text{O } J = 1-0$  observations, an upper limit to the mean column density of the tail is  $1 \times 10^{21} \text{ cm}^{-2}$ , which is sufficient to self-shield the molecular material within the tail from the diffuse UV field.

The hydrostatic equilibrium of the tail is evaluated from the properties of the molecular and ionized gas components derived in § 3 assuming that the tail is not self-gravitationally bound. The external pressure  $P_{\text{II}}/k$  provided by the ambient, hot, ionized plasma within the chimney is  $\approx 4 \times 10^4 \text{ cm}^{-3} \text{ K}$ . The density of molecular material within the tail is estimated from the mean column density and projected width of the tail to be  $80 \text{ cm}^{-3}$ . However, if the material is inhomogeneously distributed as typically observed within the molecular ISM, the density of molecular gas within the tail could be higher. An upper limit to the gas density of the tail is  $\approx 1000 \text{ cm}^{-3}$  based on the densities required to excite  $\text{C}^{18}\text{O } J = 1-0$  emission and a large velocity gradient modeling of the observed upper limits of  $\text{CS } J = 2-1$  emissions from the base of the tail region. Assuming a kinetic temperature of  $10 \text{ K}$ ,  $P/k$  may range from  $800$  to  $10^4 \text{ cm}^{-3} \text{ K}$ . Thus, it is plausible that the cometary tail is compressed by the pressure of the external gas, which may account for the small width of the tail relative to the presumed umbra cast by the head of the cometary cloud.

The primary effect of the shock front is the implosion of material to the symmetry axis of the cloud. Thus, one would expect the accumulation of large amounts of material within a limited volume. Such high-density conditions are conducive to the formation of additional massive stars. IRAS PSC 02310+6133 attests to recent star formation within the head of the cometary cloud. While the exact location of the shock front is not accurately identified from these observations, the newborn star is positioned near the ionization front that trails the shock front. Moreover, the observed fan-shaped morphology of the  $\text{C}^{18}\text{O}$  and  $\text{CS}$  emissions is remarkably congruent with the simulations of Lazareff & Lefloch (1994) at the  $1.8 \times 10^5$  yr time step. If these models are applicable to this cloud, then there is a reasonable amount of time for a star to form within the imploded core.

This work was supported by NSF grant AST 94-20159 to the Five College Radio Astronomy Observatory and NASA NAG 5-28916. The *IRAS* data were processed using the CSCC parallel computer system operated by Caltech on behalf of the Concurrent Supercomputing Consortium. Access to this facility was provided by Caltech.

#### REFERENCES

- Alter, G., Ruprecht, J., & Vanysek, V. 1970, *Catalog of Star Clusters and Associations* (2d ed.; Budapest: Akademiai Kiado)
- Bertoldi, F. 1989, *ApJ*, 346, 735
- Bertoldi, F., & McKee, C. F. 1990, *ApJ*, 354, 529
- Cao, Y., Prince, T. A., Terebey, S., & Beichman, C. A. 1996, *PASP*, in press
- Heyer, M. H. 1996, in *CO: Twenty Five Years of Millimeter Wave Spectroscopy*, ed. W. Latter, D. Emerson, & S. Radford (Dordrecht: Kluwer), in press
- IRAS Point Source Catalog, Version 2*. 1988, Joint *IRAS Science Working Group* (Washington: GPO)
- Lefloch, B., & Lazareff, B. 1994, *A&A*, 289, 559
- Massey, P., Johnson, K. E., & DeGioia-Eastwood, K. 1995, *ApJ*, 454, 151
- Mezger, P. G., & Henderson, A. P. 1967, *ApJ*, 147, 471
- Normandeau, M., Taylor, A. R., & Dewdney, P. 1996a, *Nature*, in press
- . 1996b, *A&AS*, submitted
- Oort, J. H., & Spitzer, L. 1955, *ApJ*, 121, 6
- Panagia, N. 1973, *AJ*, 78, 929
- Serabyn, E., Güsten, R., & Mundy, L. 1993, *ApJ*, 404, 247
- Spitzer, L. 1978, *Physical Processes in the Interstellar Medium* (New York: Wiley)
- Strong, A. W., et al. 1988, *A&A*, 207, 1
- Sugitani, K., Fukui, Y., & Ogura, K. 1991, *ApJS*, 77, 59
- Westerhout, G. H. 1958, *Bull. Astron. Inst. Netherlands*, 14, 215

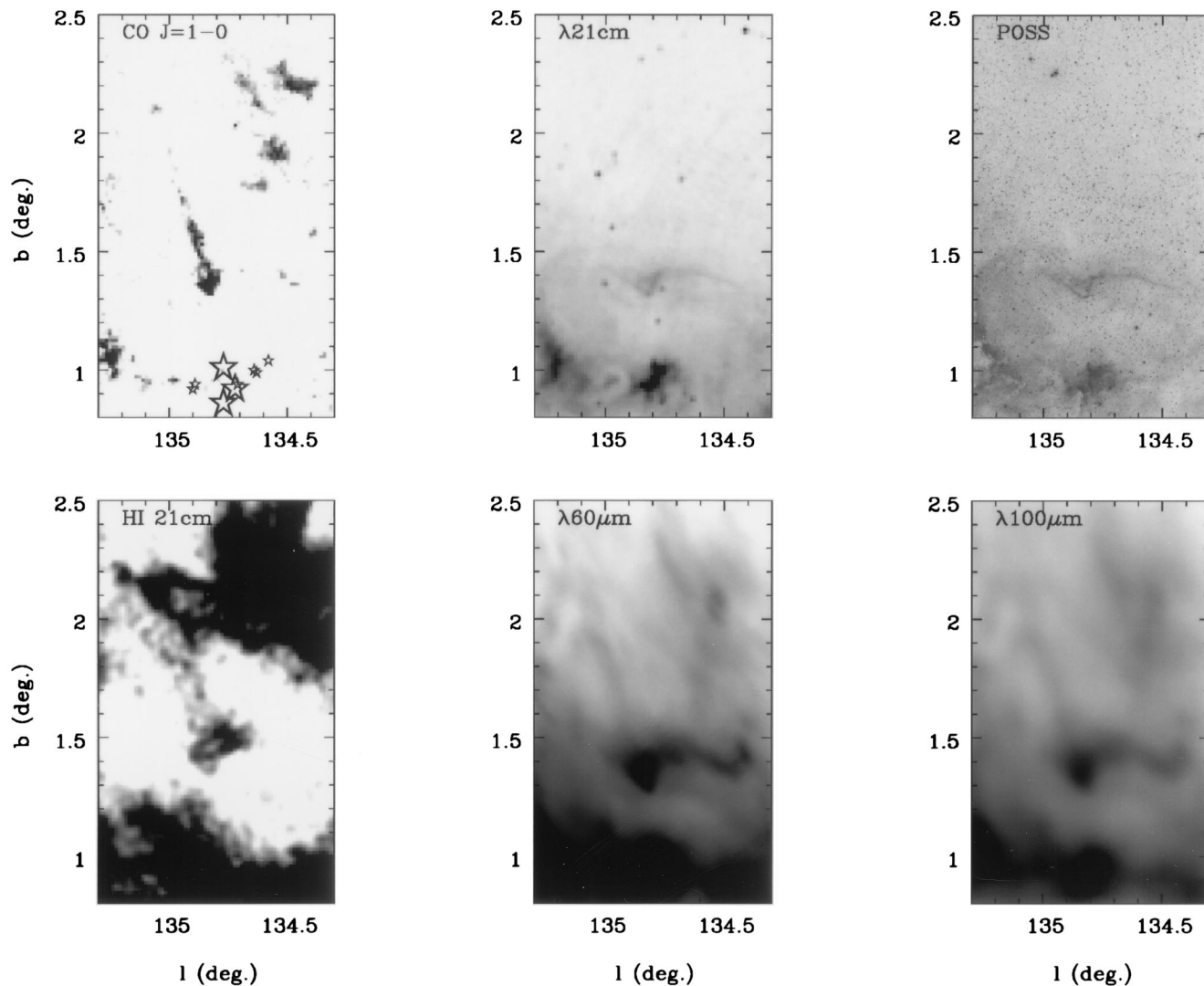


FIG. 1.—Mosaic of the cometary cloud as imaged by several probes of the interstellar gas and dust components. Clockwise from the upper left: integrated  $^{12}\text{CO}$   $J = 1-0$  emission over the velocities  $-42.5$  to  $-37.5$   $\text{km s}^{-1}$  with halftones ranging from 1 to 15  $\text{K km s}^{-1}$ —the three large open stars mark the positions of the most luminous sources of ionizing photons, and the smaller open stars mark the positions of the remaining members of the compact group of O stars of IC 1805; 21 cm radio continuum emission with halftones from 1 to 50 K; Palomar Sky Survey Red Plate; 100  $\mu\text{m}$  *IRAS* co-added image with logarithmic halftones between 32 and 320  $\text{MJy sr}^{-1}$ ; 60  $\mu\text{m}$  *IRAS* co-added image with logarithmic halftones between 10 and 100  $\text{MJy sr}^{-1}$ ; integrated H I 21 cm residual line emission over the velocities  $-42.5$  to  $-37.5$   $\text{km s}^{-1}$  with halftones ranging from 50 to 250  $\text{K km s}^{-1}$ .

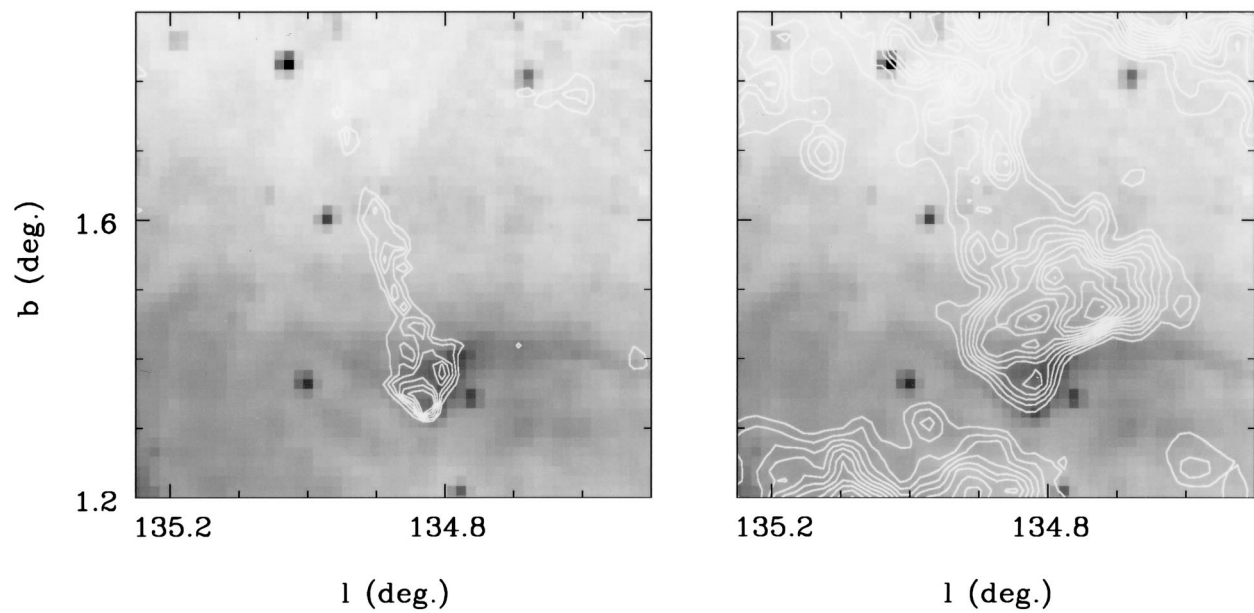


FIG. 3.—*Left*: contours of integrated  $^{12}\text{CO } J=1-0$  overlaid upon the 21 cm continuum image. *Right*: contours of integrated H I 21 cm line emission overlaid upon the 21 cm continuum image. These images show the spatial relationship among the molecular, atomic, and ionized gas components.

ERRATUM

In the Letter "A Massive Cometary Cloud Associated with IC 1805" by Mark H. Heyer, Christopher Brunt, Ronald L. Snell, John Howe, F. P. Schloerb, John M. Carpenter, M. Normandeau, A. R. Taylor, P. E. Dewdney, Y. Cao, S. Terebey, and C. A. Beichman (ApJ, 464, L175 [1996]), Figure 2 contains a graphical error resulting from a mismatch of the image with respect to the grid values. The correct version of Figure 2 is reproduced below.

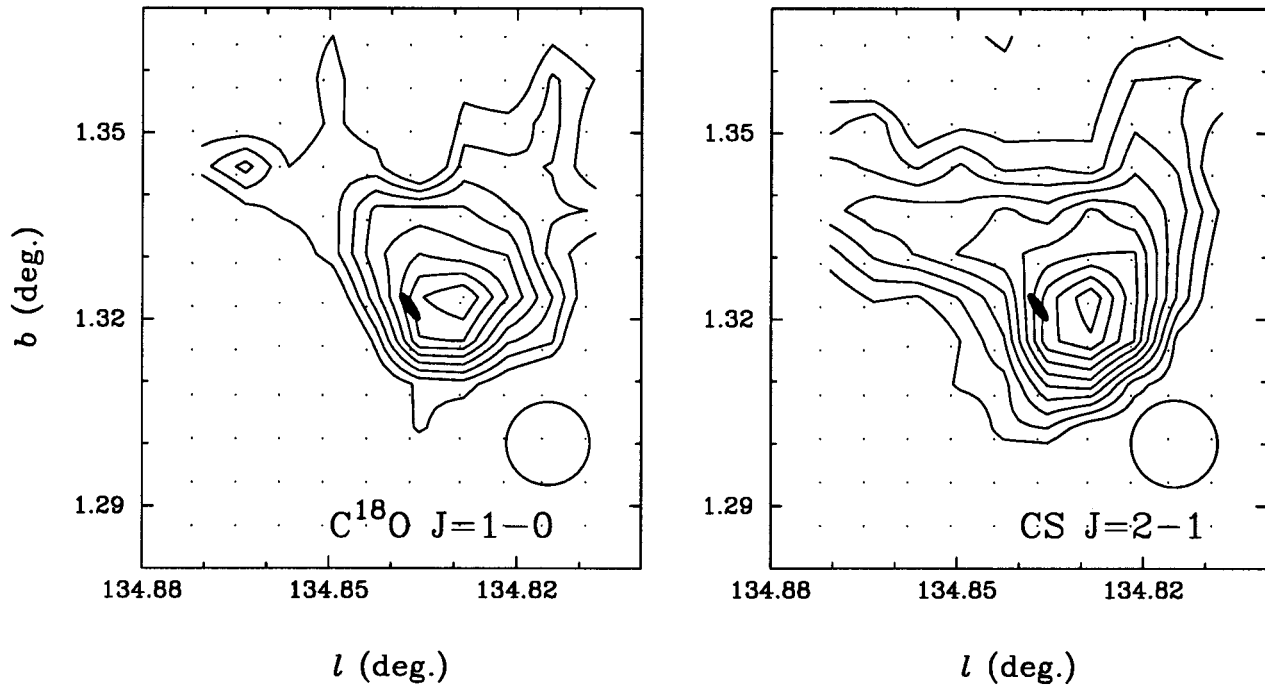


FIG. 2.—Maps of main-beam integrated  $C^{18}O\ J=1-0$  (left) and  $CS\ J=2-1$  (right) emission. For the  $C^{18}O$  map, the contours are 0.6–2.7, spaced by  $0.3\ \text{K km s}^{-1}$ . The contours for the CS map are 0.3–1.8, spaced by  $0.3\ \text{K km s}^{-1}$ . The filled ellipse denotes the location and positional uncertainty (95% confidence level) of IRAS PSC 02310+6133, the small dots show the mapped points, and the circle denotes the observed beam size.